MVA'90 IAPR Workshop on Machine Vision Applications Nov. 28-30,1990, Tokyo

AN ADAPTIVE ALGORITHM FOR EDGE DETECTION WITH SUBPIXEL ACCURACY IN NOISY IMAGES

Jesse S. Jin
AI Lab, Computer Science Department
University of Otago

P. O. Box 56, Dunedin
New Zealand

ABSTRACT

There is a tradeoff between noise insensitivity and accurate position in edge detection. This paper suggests an adaptive algorithm which takes advantage of both LoG and NonLL filters. Several masks of different size cover a wide band of frequencies under the supervision of the nonlinear Laplace filter. Calculation is dramatically reduced by thresholding. Zero-crossings are tested simultaneously with convolution and interpolated with subpixel accuracy.

INTRODUCTION

The earliest and most popular spatial differentiation in visual information processing began with the gradient operator. The absolute value of the first derivative is maximal near the position of the steepest descent where the second derivative (Laplacian) crosses zero[Davis75]. The Laplacian operator was nearly abandoned due to noise sensitivity and phantom edges when Kelly suggested a blurred Laplacian for retinal modeling of psychophysical results and Marr suggested Laplacian following multiple scales of Gaussian blurring[Daugman88,Marr82]. Neural receptive fields take profiles resemble the Laplacian of Gaussian(LoG), which achieves the lowest bound on the joint entropy. It is equivalent to the minimal product of the varriances in both the spatial and the spatial frequency domain[Olshausen88].

The filter sensitivity is associated with the width of the central excitatory region of LoG. A large σ, corresponding to a large Gaussian filter, can be used to find strong edges with approximate position, while a small σ can be used to obtain more detail edges with high positional accuracy. There is a tradeoff between noise insensitivity and accurate position in choosing the size of filter[Canny83].A further consideration comes from a computational point of view on the large Marr-Hildreth filter. Although the filters can be decomposed into seperate row and column filters, the calculation is still considerable high and there is another constraint requiring the sum of the resulting filter coefficients is zero. However, later work suggests that zero-crossings of the Laplacian are not the only features computed in early vision[Torre86]. Level-crossings, which result from convolution with a non-zero coefficient filter, are quite useful in detecting some special frequencies[Daugman88].The experiment discovers that a nonlinear Laplacian filter(NonLL) can greatly reduce the size of filter with high tolerance to noise, which means that the product of variances in both the spatial and the spatial frequency domain is smaller than the limit of LoG. It may be possible to separate automatically the noise response and the real edge response for medium and high signal to noise ratios using the threshold selection algorithm available, but it is hard to find an algorithm robust enough for images with low signal to noise ratio[Vliet89].

Another saving of calculation is obtained by reducing the sampling frequency,that is reducing the resolution. Convolution is done using a small filter. A subpixel edge detection scheme is used to recover the edges at the original resolution[Huertas86]. Its foundation is that human beings are able to recognize objects starting from a very crude outline[Vliet89].

We suggest a scheme combining LoG with NonLL filters. Different size of LoG filters are chosen under the guide of NonLL output. Calculation is dramatically reduced by thresholding. Zero-crossings are tested simultaneously with convolution and interpolated with subpixel accuracy.

FREQUENCY ANALYSIS OF LOG AND NONLL FILTERS

The photoreceptors tend to have a central excitatory region, which takes a profile of Gaussian. Ganglion cell receptive fields have central/surround profile, which function as a Laplacian operator[Grimson80]. Since both filters are linear and shift-invariant they can be combined into one filter, the LoG filter[Hildreth83]. In two dimension, it is

$$\nabla^2 G(x,y) = \frac{1}{2\pi\sigma^4}\left(2 - \frac{x^2+y^2}{\sigma^2}\right)\exp\left(-\frac{x^2+y^2}{2\sigma^2}\right) \quad (1)$$

with Fourier transform:

$$\frac{1}{2\pi}\omega^2 \exp(-\frac{\omega^2\sigma^2}{2}) \qquad (2)$$

Here $\omega = 2\pi f$ is a bandpass filter with a maximum at $\omega = \frac{\sqrt{2}}{\sigma}$ (see Fig. 1b). A different size of filter has a different width of the central excitatory region.

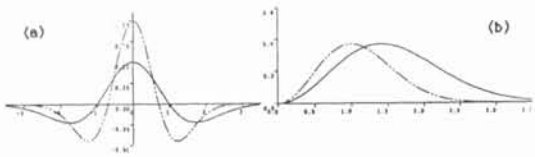

Fig. 1 LoG filters(a) and their Fourier transform(b)

For small values of σ, LoG filter extract the high frequency edges in the image with high accurate position. But the ability to suppress noise is very poor. For large values of σ, the LoG filter will extract the low frequency information. It can get rid of noise, for noise usually contains high frequency information, at the cost of poor positioning of boundaries. Fig. 2 gives two zero-crossing images with sizes equal 4 (a) and 17 (b) respectively.

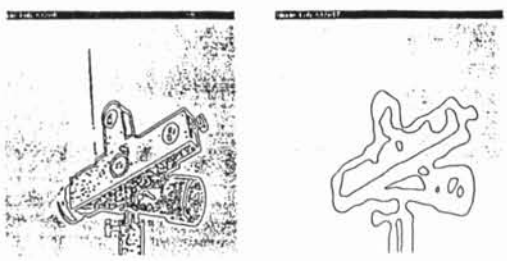

Fig.2 zero-crossings with filter size 4(a) and 17(b)

Another approach to simulating the central excitatory profile is the design of a nonlinear Laplacian. Filtered with a low-pass filter, images are convolved with Laplacian operator by a nonlinear combination of neighborhood pixels[Rosenfeld70]. One low-pass filter used in nonlinear Laplacian is the averaging filter. Fig. 3 gives the amplitude-frequency response curves of Gaussian filter and averaging filter. From the spectrum we can see that there are still peak values after the main wave, which means that there are still some frequencies passing through. It is also noticed that the energy of the low frequencies is reduced due to extending wave peaks. That is to say, it reduces the energy of edges. Rosenfeld suggested a nonlinear low-pass filter, the median filter[Rosenfeld82]. Filtered output is the median value within the mask.

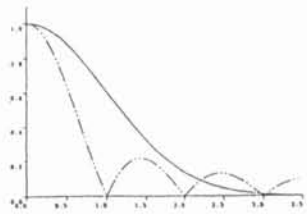

Fig3. Amplitude-frequency response
(Solid line: Gaussian; dashed line: averaging)

Although it is difficult to give exactly the amplitude-frequency response characteristic, which is a function of distribution of intensity, two characteristics are obvious. One is that it preserves the energy of edges. Another one, according to the law of large numbers, is that it approximates the Gaussian function when the size of mask is big enough.

IMPLEMENTATION OF ADAPTIVE FILTERING

For an n × n neighborhood, we define a new nonlinear Laplace filter, NonLL, by

$$\text{NonLL}(x,y) = \text{gradmax}(x,y) + \text{gradmin}(x,y) \quad (3)$$

where

$$\text{gradmax}(x,y) = \max\{C_n(x',y')[I(x',y') - \frac{I(x,y)+\text{median}(x,y)}{2}]\}$$

$$\text{gradmin}(x,y) = \min\{C_n(x',y')[I(x',y') - \frac{I(x,y)+\text{median}(x,y)}{2}]\}$$

$$(x',y') \in d_n(x,y) \quad (4)$$

$d_n(x,y)$ is an n × n square centered at (x,y), $C_n(x',y')$ are scale coefficients for the position and median(x, y) is median value within n × n neighbors. This new filter performs smoothing and Laplacian operations in one pass. Edges are extracted by thresholding over min(gradmax, -gradmin). Fig. 2 gives a picture (a) and its co-occurrence spectrum(b). From the spectrum, we can see the distribution of gradient. The diagonal elements construct the histogram of the image. The diagonal distribution is the distribution of gradient. Threshold is set by

isolating the diagonal cluster sets. Only the points above threshold need to search for zero-crossings. Generally speaking, a large gradient corresponds to a high frequence edge. We choose LoG size after thresholding NonLL. Due to its symmetry, the discrete filter of equation can be rewritten as a combination of two separable filters:

$$\nabla^2 G(x,y) = h_1(x)h_2(y) + h_2(x)h_1(y) \qquad (5)$$

$$= \frac{1}{2\pi\sigma^4} \sum_{m=-\infty}^{\infty} \left(1-\frac{m^2}{\sigma^2}\right) \exp\left(\frac{m^2}{\sigma^2}\right) \sum_{n=-\infty}^{\infty} \exp\left(-\frac{n^2}{2\sigma^2}\right)$$

$$+ \frac{1}{2\pi\sigma^4} \sum_{m=-\infty}^{\infty} \exp\left(-\frac{m^2}{2\sigma^2}\right) \sum_{n=-\infty}^{\infty} \left(1-\frac{n^2}{\sigma^2}\right) \exp\left(-\frac{\nu^2}{\sigma^2}\right)$$

It can be seen from Fig. 2(b) that a lot of calculation is saved by thresholding. m and n are truncated to N giving a FIR[Oppenheim75], under the constraint

$$\sum_{m=-N}^{N} h_1^{(N)}(m) \sum_{n=-M}^{M} h_2^{(N)}(n) = 0 \qquad (6)$$

where $h_1^{(N)}(k)$ and $h_2^{(N)}(k)$, and different sizes of filter respond to different value of gradient. It is worthy mentioning that if this algorithm is used for testing level-crossings, equation (6) changes to

$$\sum_{m=-N}^{N} h_1^{(N)}(m) \sum_{n=-M}^{M} h_2^{(N)}(n) = a^{(N)} \qquad (7)$$

Here $a^{(N)}$ are level constants and have the same sign for all filters.

ZERO-CROSSING DETECTION AND INTERPOLATION

All zero-crossing detection algorithms used in the references were proceeded after convolution. It obviously reduces speed. We found it not necessary, for we only need to test zero-crossings with 180 degree. Fig. 4 gives the data structure and illustrates testing strategy. For an n × n image, we define an array with n+1 elements to hold a testing boundary. Directions 8, 1, 2 and 3 are tested for each pixel, as indicated in Fig. 4(a). After being used to test zero-crossings, the convolution result is put into the left top of testing boundary as the arrow points out. The test boundary shifts one element right each line and all n+1 elements are wrapped up for continuous testing.

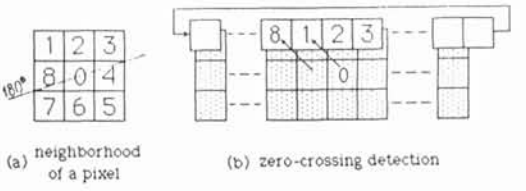

Fig.4 Data structure for zero-crossing detection

Because large σ LoG filters are required to suppress noise, it is very time-consuming to do convolution. However, we can reduce the resolution of images and use filters of small σ upon low resolution images. Then we use a subpixel edge detection scheme to recover the edges at the original resolution. Subpixel values of zero-crossing localization are obtained by a polynomial interpolating function. All convolutions are performed using floating-point arithmetic in our implementation. The approximate interpolating function is written as

$$x' = \frac{x_2 f(x_1,y_1) - x_1 f(x_2,y_2)}{f(x_1,y_1) - f(x_2,y_2)} \quad \text{if } x_1 \neq x_2 \qquad (8)$$

$$y' = \frac{y_2 f(x_1,y_1) - y_1 f(x_2,y_2)}{f(x_1,y_1) - f(x_2,y_2)} \quad \text{if } y_1 \neq y_2 \qquad (9)$$

where f(x, y) is the value of the LoG filter output. The (x', y')s are used aspoints for later interpolation which we suggest in the form

$$y \approx \sum_{i=k}^{k+2} \left(\prod_{j=k, j\neq i}^{k+2} \frac{x-x_j}{x_i-x_j}\right) y_i \qquad (10)$$

The subpixel accuracy can be any resolution, but the higher resolution, the lower the accuracy of approximation.

CONCLUSION

Canny has distinguished three performance criteria in judging the ability of an algorithm to find an edge: good detection, good localization and only one response to a single edge. We give the fourth criterion, execution speed. Our edge detector performs well over these four criteria. It increases

speed more than ten times and can work at very low signal-to-noise ratios, as shown in Fig. 5

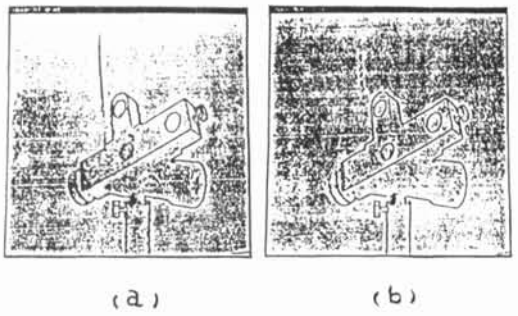

Fig. 5 Results: (a)threshold output; (b)zero-crossings

Recent information processing in visual systems has shown that zero-crossings in the band passed signals do not capture the necessary information in some patterns, so level-crossings are suggested. Our algorithm can be used for detecting level-crossings without any big changes. Fig. 6 gives a texture image generated by Daugman, its zero-crossings and level-crossings.

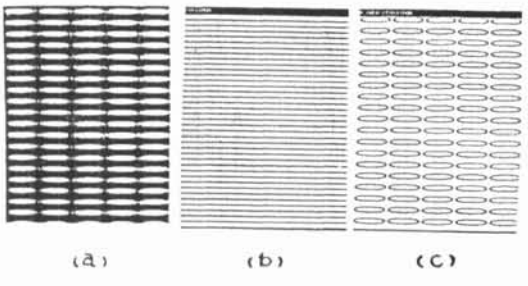

Fig. 6 Texture image(a)
its zero-crossings(b) and level-crossings(c)

Extracting more information from images is a topic of further research[Porat88].

ACKNOWLEDGMENTS

This research was supervised by Prof. B. G. Cox, Dr. W. K. Yeap and Dr. M. Alexander, and funded by University Grants Committee, New Zealand.

REFERENCES

[Canny83]J.F. Canny. Finding edges and lines in images. PhD thesis, MIT, June 1983.

[Daugman88]J.G. Daugman. Pattern and motion vision without laplacian zero crossings. J. Opt. Soc. Am. A, 5(7):1142--1148, 1988.

[Davis75]L.S. Davis. A survey of edge detection techniques. Comput. Graphics Image Processing, 4:248--70, 1975.

[Grimson80]W.E.L. Grimson. A computer implementation of a theory of human stereo vision]. PhD thesis, MIT, January 1980.

[Hildreth83]E.C. Hildreth. The detection of intensity changes by computer and biological vision systems. Comput. Vision Graphics Image Processing, 22:1--27, 1983.

[Huertas86]A.Huertas and G.Medioni. Detection of intensity changes with subpixel accuracy using laplacian-gaussian masks. IEEE T-PAMI, PAMI-8(5):651--64, 1986.

[Marr82]D.Marr. Vision. Freeman, New York, 1982.

[Olshausen88]B.A. Olshausen. A survey of visual preprocessing and shape representation techniques. PhD thesis, RIACS Technical Report 88.35, 1988.

[Oppenheim75]A.V. Oppenheim and R.W. Schafer. Digital Signal Processing. Englewood Cliffs NJ Prentice-Hall, 1975.

[Porat88]Moshe Porat and YehoshuaY. Zeevi. The generalized gabor scheme of image representation in biological and machine vision. IEEE T-PAMI, 10(4):452--68, 1988.

[Rosenfeld70]A.Rosenfeld. A nonlinear edge detection technique. Proc. IEEE, 58:814--6, 1970.

[Rosenfeld82]A.Rosenfeld and A.C. Kak. Digital Picture Processing, volume1. Academic Press, 1982.

[Torre86]V.Torre and T.Poggio. On edge detection. IEEE T-PAMI, PAMI-8:147--63, 1986.

[Vliet89]L.J.Van Vliet and I.Young. A nonlinear laplace operator as edge detector in noisy images. Comput. Vision Graphics Image Processing, 45(1):167--95, 1989.